Journal of Alloys and Compounds 371 (2004) 129–132

Journal of ALLOYS AND COMPOUNDS

www.elsevier.com/locate/jallcom

ZnO–GaN tunnel junction for transparent ohmic contacts to p-GaN

E. Kaminska [a,*], A. Piotrowska [a], K. Golaszewska [a], R. Kruszka [a], A. Kuchuk [a], J. Szade [b], A. Winiarski [b], J. Jasinski [c], Z. Liliental-Weber [c]

[a] *Institute of Electron Technology, Al. Lotników 32/46, Warsaw 02-668, Poland*
[b] *University of Silesia, Katowice, Poland*
[c] *Lawrence Berkeley National Laboratory, Berkeley, CA, USA*

Received 19 November 2002; received in revised form 12 June 2003; accepted 13 June 2003

Abstract

The fabrication procedure of transparent n^+-ZnO–p-GaN ohmic junctions has been described. The influence of consecutive technological steps on the electrical, structural and electronic properties of the junction has been studied. The results indicate that the predeposition of Au nucleation film plays a crucial role for the final contact properties. The ohmic behaviour is explained in terms of formation of a tunnel n^+-ZnO–p-GaN junction.

PACS: 73.40 Gk; 73.40 Kp; 73.61 Ga; 79.60 Jv

Keywords: Semiconductors; Surfaces and interfaces; Scanning and transmission microscopy; Photoelectron spectroscopies

1. Introduction

GaN and ZnO, both wide-band-gap semiconductors, have recently attracted considerable world-wide interest because of their potential application in short-wavelength optoelectronics [1,2]. As for GaN, the research resulted in greatly improved epitaxial growth of GaN–AlGaN–InGaN heterostructures and their refined processing technologies. The performance of devices, however, is still limited by insufficient p-type doping followed by poor characteristics of p-type ohmic contacts. The p-type-contacting problem becomes even more acute in the case of devices requiring a transparent p-type electrode for their operation. To satisfy this, ultra thin metallizations are used, albeit at the cost of increased contact resistance [3]. Concerning ZnO, a noticeable progress in thin film growth and controlled n-type doping have been reported. However, the growth technology for conducting p-type material has not been established yet. The similarity of GaN and ZnO in terms of energy gap, crystallographic structure and high thermal stability make them attractive candidates for forming heterojunctions. Although, the data concerning electronic properties of ZnO–GaN interfaces are very scarce, both ab initio calculations [4] and band offset measurements performed on ZnO epilayers grown on GaN templates [5] emphasise the influence of the initial GaN surface structure on the final characteristics of ZnO–GaN heterojunction.

The aim of this work was to study the feasibility of fabrication of an n^+-ZnO–p-GaN tunnel junction (TJ), suitable for application as a transparent ohmic contact to p-type GaN. The use of a TJ contact instead of a conventional p-type ohmic contact has been demonstrated for GaAs-based lasers [6]. Such an approach seems especially valuable for GaN-based devices, and promising results with sputter deposited n^+-type indium tin oxide (ITO) have been reported. Although, n^+-ITO–p-GaN junctions were not ohmic [7], ITO-contacted devices [8] showed effective hole injection.

2. Experimental procedure

GaN(0 0 0 1) samples for this study were MOCVD grown on a sapphire substrate. Two micrometer thick p-GaN epilayers were Mg doped to the hole concentration of $(1-5) \times 10^{17}$ cm^{-3}. Prior to ZnO fabrication the samples were etched

* Corresponding author. Tel.: +48-2254-87942; fax: +48-2284-70631.
E-mail address: eliana@ite.waw.pl (E. Kaminska).

0925-8388/$ – see front matter © 2003 Elsevier B.V. All rights reserved.
doi:10.1016/j.jallcom.2003.06.014

in 10% $(NH_2)_2CS$:HCl:15% H_2O_2 = 20:1:1 and immediately loaded into the vacuum chamber. The surface treatment was completed by in situ Ar^+ ion sputter etching at 300 V for 30 s.

Thin ZnO films were fabricated by furnace oxidation of vacuum deposited zinc layers. To overcome the problem of non-uniform condensation of Zn on bare GaN surface, an Au nucleation film was predeposited. Thermal evaporation of Au was optimised such as to obtain a non-continuous film with island-like structure providing nucleation centres for homogeneous deposition of Zn. The morphology of the Au nucleation films was examined with an atomic force microscope. Sixty nanometers thick Zn layers were deposited by thermal evaporation and oxidised in O_2 flow, at 320 °C for 40 min. Their thickness increased to 80 nm upon annealing.

Optical transmission was measured by photospectrometry, using ZnO films deposited onto back-side polished sapphire. ZnO conductivity was assessed from four-point probe and van der Pauw measurements. Specific resistance r_c of n^+-ZnO–p-GaN junctions were determined by the circular transmission line method (CTLM) [9]. The following dimensions of the CTLM structure were used: $r = 50\,\mu m$ and spacings 10, 20, 30, 45, and 60 μm. For electrical characterisation purposes, Au pads were deposited on the ZnO surface. It has been proven that Au forms a low resistivity ohmic contact with n-ZnO. Patterns for electrical measurements were fabricated by lift-off photolithography.

The microstructure of the ZnO–GaN interface was investigated by cross-sectional transmission electron microscopy (XTEM) and high resolution imaging (HREM). TEM observations were performed using a Topcon 002 B microscope operating at 200 keV.

X-ray photoemission spectroscopy (XPS) was applied for the study of electronic properties of p-GaN surface and n^+-ZnO–p-GaN interface. The measurements were performed with a Physical Electronics PHI 5700 ESCA spectrometer, at a pressure $\sim 10^{-10}$ Torr, using monochromatised Al Kα (1486.6 eV) and non-monochromatised Mg Kα (1256 eV) radiation, respectively. The atomic composition was obtained from Mg radiation spectra as for Al radiation the N (1s) line overlaps with the Ga LMM Auger lines. The energy calibration was verified using the Fermi level edge or C (1s) line for conducting or non-conducting samples, respectively. The contamination with carbon, originating from the air exposure of the sample surface, usually leads to the appearance of the line at 284.6 eV.

3. Results and discussion

The conductivity of ZnO films strongly depends on the process parameters of Zn deposition. Zn deposited at a pressure 1×10^{-5} Pa forms, under oxidation, highly resistive ZnO. By increasing the working pressure during Zn evaporation above 10^{-4} Pa, by back-filling the deposition chamber with high-purity N_2, conducting ZnO films have been obtained. Zn films deposited at $(1.5-6.5) \times 10^{-3}$ Pa yield after oxidation half-metallic n-type ZnO with a free carrier concentration $n \geq 10^{20}\,cm^{-3}$ and resistivity $\rho < 10^{-3}\,\Omega\,cm$. Their optical transmission in the wavelength range from 400 to 700 nm exceeds 70%.

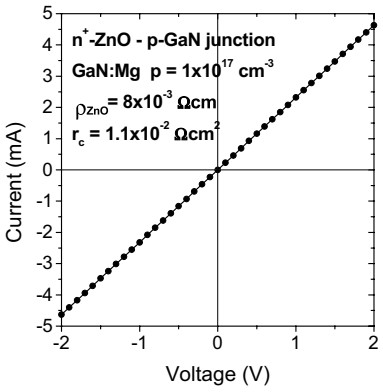

Fig. 1. *I–V* characteristic for n^+-ZnO–p-GaN ohmic junction.

To evaluate the electrical properties of ZnO–GaN junctions, first the effect of Au has been examined. For this purpose *I–V* characteristics of pure Au (100 nm thick) and Au/Zn (Au nucleation film/60 nm Zn) contacts on p-GaN have been measured and found to be non-ohmic. Regarding n-ZnO–p-GaN junctions, n-ZnO overlayers of a resistivity above $10^{-2}\,\Omega\,cm$ produce rectifying junctions. The onset of the ohmic behaviour with linear *I–V* characteristics, Fig. 1, is observed for $\rho \approx 10^{-2}\,\Omega\,cm$, and corresponds to the specific junction resistance of $r_c \approx 1 \times 10^{-2}\,\Omega\,cm^2$. By using half-metallic ZnO ($\rho < 1 \times 10^{-3}\,\Omega\,cm$) it was possible to decrease r_c to $5 \times 10^{-4}\,\Omega\,cm^2$.

The XTEM micrograph of ZnO–GaN interface, presented in Fig. 2a, gives evidence that the ZnO fabrication does not alter the microstructure of GaN sub-contact region. The interface is abrupt with no sign of reaction (Fig. 2a). The upper part of the junction is composed of two distinct phases. HREM analysis assisted by fast Fourier transform procedure (FFT) have been used to identify dark islands embedded in a light-coloured film as crystalline Au dots (Fig. 2b) set in polycrystalline hexagonal zinc oxide film (Fig. 2c). The Au coverage of the GaN surface is about 40%. Note that the nonhomogeneous contrast in the TEM micrographs comes from the non-uniform thickness of the cross-sectional specimen, resultant from the specimen thinning procedure by ion milling.

Fig. 3 shows the parts of the photoemission spectra corresponding to the binding energy from 0 to 25 eV, acquired after consecutive steps of n-ZnO–p-GaN junction fabrication. The binding energy range was chosen such as to include the Ga (3d) and the Zn (3d) core level peaks. The double peak in spectra labelled b, c and e at the binding energy range 2–8 eV, comes from Au (5d) states. Regarding Zn, the Zn (3d) core level in the spectrum d, appears in a higher binding energy position as compared to the spectrum c, indicating

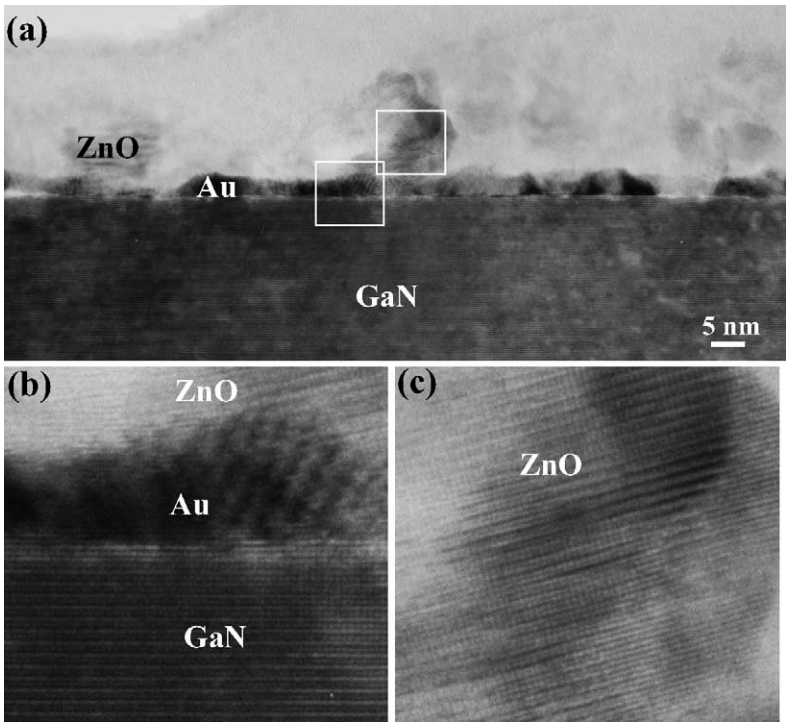

Fig. 2. XTEM micrographs of GaN–ZnO interface: (a) TEM image of the interface, (b) and (c) HREM images of crystalline Au and ZnO phases.

that zinc has reacted with oxygen. Since the original ZnO film was too thick for assessing Ga (3d) core level (spectrum d), in situ sputter thinning was performed enabling observation of both, Ga (3d) and Zn (3d) core levels (spectrum e). It should be noted that neither the shape of the Zn (3d) peak nor its position has been altered by the process of sputter thinning.

The displacement of the binding energy of Ga (3d) core level, being the measure of the Fermi level shift at the GaN surface [10], corresponds to the band bending at the interface caused by the given technological step. In the spectrum labelled a, representative of a clean p-GaN surface, the Ga (3d) peak is centred at 19.6 eV, which compares well with values 19 [11] and 20 eV [12] reported for similar p-GaN samples. The gradual shift of the position of Ga (3d) core level to higher binding energies, resulting from subsequent deposition of Au and Zn, followed by Zn oxidation indicates the pulling of the Fermi level at the interface towards the conduction band edge. Careful measurements indicate that the Fermi level moves by ∼0.7 eV after deposition of Au nucleation film. Zn overcoat induces additional shift by 0.1 eV. Oxidation of Zn film causes further displacement of the Fermi level by 0.4 eV. Thus, the total movement of Fermi level due to the formation of n-ZnO on p-GaN surface corresponds to a downward band bending by ∼1.2 eV.

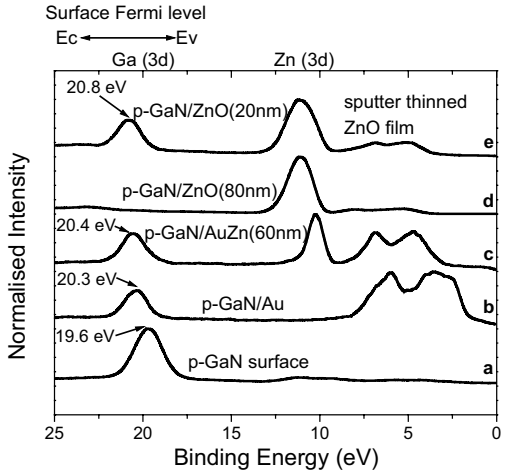

Fig. 3. Photoemission spectra of Ga (3d) and Zn (3d) core levels for the initial p-GaN surface and after consecutive steps of ZnO fabrication.

It is important to note, that the binding energy of the Au ($4f_{7/2}$) core level after deposition of the Au nucleation film was 84 eV, which corresponds to clean, metallic gold. This indicates that no interaction has occurred at the GaN–Au interface.

4. Conclusions

We have described the fabrication procedure of transparent n^+-ZnO films enabling to form ohmic contacts to low-doped p-GaN. While high ZnO conductivity might be attributed to the defects caused by nitrogen atoms introduced during Zn deposition, XPS gave evidence of particularly strong consequence of the Au predeposition for the downward band bending at p-type GaN surface, accompanying

the formation of n-ZnO–p-GaN interface. Electrical measurements clearly indicate that neither pure Au nor Au/Zn do form ohmic contact to p-GaN.

Another point to be taken into consideration deals with surface properties of n^+-ZnO. Recently published data on transparent conducting oxides (TCOs) indicate that in spite of highly doped bulk, TCOs develop a substantial depletion layer at the surface [13]. A similar behaviour at the ZnO side of the interface could be expected. Resultant upward band bending together with the enhanced downward band bending at p-GaN side would explain the observed ohmic behaviour in terms of a tunnel n^+-ZnO–p-GaN junction.

Acknowledgements

Research is partially supported by grants from European Commission IST-1999-10292-AGETHA and by the Director, Office of Science, Office of Basic Energy Sciences, Division of Materials Sciences, of the US. Department of Energy under Contract No. DE-AC03-76SF00098.

References

[1] S. Nakamura, G. Fasol, Springer, 1997.
[2] J.E. Nause, III–V Review 12 (1999) 28.
[3] J.S. Jang, S.J. Park, T.Y. Seong, J. Appl. Phys. 88 (2000) 5490.
[4] T. Nakayama, M. Murayama, J. Cryst. Growth 214–215 (2000) 299.
[5] S.K. Hong, T. Hanada, H. Makino, H.J. Ko, Y. Chen, T. Yao, J. Vac. Sci. Technol. B 19 (2001) 1429.
[6] J.J. Wierer, P.W. Evans, N. Holonyak, D.A. Kellogg, Appl. Phys. Lett. 71 (1997) 3468.
[7] J.K. Sheu, G.C. Chi, M.J. Jou, C.M. Chang, Appl. Phys. Lett. 72 (1998) 3317.
[8] T. Margalith, O. Buchinsky, D.A. Cohen, A.C. Abare, M. Hansen, S.P. DenBaars, L.A. Coldren, Appl. Phys. Lett. 74 (1999) 3930.
[9] G.S. Marlow, M.B. Das, Solid-State Electron. 25 (1982) 91.
[10] J. Sun, D.J. Seo, W.L. O'Brien, F.J. Himpsel, A.B. Ellis, T.F. Kuech, J. Appl. Phys. 85 (1999) 969.
[11] D.-W. Kim, J.C. Bae, W.J. Kim, H.K. Baik, J.M. Myoung, S.-M. Lee, J. Electron. Mater. 30 (2001) 183.
[12] J. Sun, K.A. Ricket, J.M. Redwing, A.B. Ellis, T.F. Kuech, Appl. Phys. Lett. 76 (2000) 415.
[13] A. Klein, Appl. Phys. Lett. 77 (2000) 2009.